Title

Community structure explains antibiotic resistance gene dynamics over a temperature gradient in soil

Authors

TK Dunivin[1,2] and A Shade[1,3, 4]

[1]Department of Microbiology and Molecular Genetics, Michigan State University, East Lansing, MI 48824

[2]Environmental and Integrative Toxicological Sciences Doctoral Program, Michigan State University, East Lansing 48824

[3]Program in Ecology, Evolutionary Biology and Behavior, Michigan State University, East Lansing, MI 48824

[4]Department of Plant, Soil, and Microbial Sciences, Michigan State University, East Lansing MI 48824

* Correspondence:

Ashley Shade

shadeash@msu.edu

Abstract

Soils are reservoirs of antibiotic resistance genes, but dynamics of antibiotic resistance genes in the environment are largely unknown. Long-term disturbances offer extended opportunities to examine microbiome responses at scales relevant for both ecological and evolutionary processes,

PeerJ Preprints | https://doi.org/10.7287/peerj.preprints.3484v1 | CC BY 4.0 Open Access | rec: 22 Dec 2017, publ: 22 Dec 2017

and therefore can be insightful for studying the dynamics of antibiotic resistance genes in the environment. We examined antibiotic resistance genes in soils overlying the underground coal seam fire in Centralia, PA, which has been burning since 1962. As the fire progresses, previously hot soils can recover to ambient temperatures, which creates a gradient of contemporary and historical fire impact. We examined metagenomes from fire-affected, recovered, and reference surface soils to examine gene-resolved dynamics of antibiotic resistance using a gene-targeted assembler. We targeted 35 distinct types of clinically-relevant antibiotic resistance genes and two horizontal gene transfer-related genes (*intI* and *repA*). We detected 17 antibiotic resistance genes in Centralia, including AAC6-Ia, *adeB*, *bla_A*, *bla_B*, *bla_C*, *cmlA*, *dfra12*, *intI*, *sul2*, *tetA*, *tetW*, *tetX*, *tolC*, *vanA*, *vanH*, *vanX*, and *vanZ*. The diversity and abundance of several antibiotic resistance genes (*bla_A*, *bla_B*, *dfra12*, *tolC*) decreased with soil temperature, and changes in ARGs could largely be explained by associated changes in community structure. We also observed sequence-specific dynamics along the temperature gradient and observed compositional shifts in *bla_A*, *dfra12*, and *intI*. These results suggest that increased temperatures can reduce soil antibiotic resistance genes but that this is largely due to a concomitant reduction in community-level diversity.

Keywords

Thermophile, gene-targeted assembly, metagenome, *rplB,* coal fire

Introduction

The dissemination of antibiotic resistance genes (ARGs) is a pressing public health concern. The One Health initiative recognizes the intrinsic link between evolution of bacterial

PeerJ Preprints | https://doi.org/10.7287/peerj.preprints.3484v1 | CC BY 4.0 Open Access | rec: 22 Dec 2017, publ: 22 Dec 2017

resistance in clinical and environmental settings (Kahn 2016). Clinically relevant antibiotic resistance genes (ARGs) have been detected in "pristine environments" (Lang *et al.* 2010) as well as a variety of marine, plant, and soil microbiomes (Fierer *et al.* 2012; Gibson, Forsberg and Dantas 2014; Wang *et al.* 2015a; Fitzpatrick and Walsh 2016). Soil is considered to be an environmental reservoir of ARGs, with greater ARG diversity than the clinic (Nesme and Simonet 2015). Despite that we can easily detect ARGs in soil, dynamics of soil ARGs are not fully understood (Allen *et al.* 2010). Understanding of the dissemination of ARGs in the environment are impeded by our modest understanding of their diversification, maintenance, and dissemination (Hiltunen, Virta and Laine 2017).

Understanding the propagation and dissemination of ARGs in soil is difficult because multiple interacting factors influence their fate (Allen *et al.* 2010; Berendonk *et al.* 2015). Perhaps most obviously, ARGs can be selected when there is environmental exposure to antibiotic (Laine, Hiltunen and Virta 2016). Environmental exposure can result from the anthropogenic use of antibiotics, for example in agriculture or via wastewater treatment outputs (Kumar *et al.* 2005; Rizzo *et al.* 2013), or it can result from environmental antibiotic production by microorganisms *in situ* (Nesme and Simonet 2015). Antibiotic exposure can kill sensitive populations and allow for propagation of resistant strains. Additionally, ARGs can be horizontally transferred (Hiltunen, Virta and Laine 2017) and are often detected on plasmids and other mobile genetic elements (Van Hoek *et al.* 2011; Pal *et al.* 2015). Thus, ARGs on mobile genetic elements may be disseminated more rapidly than through population growth alone. Furthermore, several ARGs are thought to have evolved >2 billion years ago (Aminov and Mackie 2007), and these may be maintained in the absence of selective pressure from antibiotics and transferred vertically. Another complicating factor for understanding ARG dissemination is

PeerJ Preprints | https://doi.org/10.7287/peerj.preprints.3484v1 | CC BY 4.0 Open Access | rec: 22 Dec 2017, publ: 22 Dec 2017

the influence of the dynamics of soil microbial communities. While interspecies competition can impact ARG abundance, one study of many habitats showed that abiotic soil conditions can be important drivers of ARG profiles (Fierer *et al.* 2012). Anthropogenic influences, such as nitrogen addition to the soil, also can impact ARGs (Forsberg *et al.* 2014). Similarly, studies with changing abiotic conditions, such as increased temperatures, have reported subsequent reductions in ARG abundance (Qian *et al.* 2016; Tian *et al.* 2016). In these examples and others, environmental disturbance can alter soil microbial community structure (Shade *et al.* 2012; Garner *et al.* 2016; Nunes *et al.* 2016), and then can impact local ARGs and their dissemination.

Long-term disturbances that impact multiple microbial generations can provide opportunities to investigate the dynamics of ARGs in response to environmental stress. One such disturbance is Centralia, PA, the site of an underground coal seam fire that ignited in 1962. As this town was evacuated in 1984, it also represents a post-urban ecosystem of minimal contemporary anthropogenic influence. This fire continues to advance along the coal seam, creating a gradient of contemporary and historical fire impact and allowing for observation of multiple microbial generations' responses to disturbance and their potential recovery. Surface soil microbial communities in Centralia are exposed to elevated temperatures (21-57°C) (Lee *et al.* 2017) and coal combustion pollutants (Janzen and Tobin-Janzen 2008) which include trace elements such as arsenic, copper, aluminum, and lead (Janzen and Tobin-Janzen 2008; Melody and Johnston 2015). While temperature increases are large, deposition of coal combustion pollutants occurs at a slow rate and varies based on the subsurface structure and geochemical properties of the burning coal (Janzen and Tobin-Janzen 2008). Depth of the coal seam varies from the surface to 46 m (Elick 2011). Furthermore, surface temperatures cool to ambient levels as the fire progresses, but coal combustion pollutants are not necessarily removed. Previously,

PeerJ Preprints | https://doi.org/10.7287/peerj.preprints.3484v1 | CC BY 4.0 Open Access | rec: 22 Dec 2017, publ: 22 Dec 2017

93 we observed changes in bacterial and archaeal community structure with fire history that was
94 well explained by temperature rather than soil properties such as arsenic concentration (Lee *et al.*
95 2017).

96 We leveraged the long-term disturbance in Centralia to examine ARG dynamics given
97 both the abandonment of human habitation and a the presence of multigenerational stressor for
98 the microorganisms. We investigated 12 metagenomes of microbial communities from surface
99 soils along the Centralia temperature gradient for 35 clinically-relevant ARGs conferring
100 resistance to eight classes of antibiotics, as well as multi drug efflux pumps and two HGT-
101 relevant genes *repA* and *intI*. We used gene targeted assembly of the metagenomes to capture a
102 breadth of ARG diversity. To examine the potential extent of HGT in Centralia, we asked
103 whether changes in community structure explained any changes in ARG profiles. Because we
104 previously identified changes in community structure along the stressor (Lee *et al.* 2017), we
105 also asked whether functional redundancy (e.g., different ARG sequences belonging to the same
106 resistance class) within the soil microbial community moderated the impact of a disturbance on
107 ARG profiles. Functional redundancy allows that changes in community structure can occur
108 without subsequent change in ARG abundance. Also, because we focused on clinically relevant
109 ARGs rather than potentially novel ARGs from thermophilic lineages, we hypothesized that
110 ARG abundance would decrease with temperature, as observed in other studies (Diehl and
111 Lapara 2010; Qian *et al.* 2016; Tian *et al.* 2016). We were, however, also interested in dynamics
112 of specific gene sequences and hypothesized that they may have unique responses, even within
113 the same resistance class.
114
115 **Methods**

PeerJ Preprints | https://doi.org/10.7287/peerj.preprints.3484v1 | CC BY 4.0 Open Access | rec: 22 Dec 2017, publ: 22 Dec 2017

Reference Database construction

Reference gene databases of diverse, near full length sequences were constructed using selected sequences from FunGene databases (Fish *et al.* 2013) for the following genes: AAC6-Ia, *adeB*, *ANT3*, *ANT6*, *ANT9*, *bla_A*, *bla_B*, *bla_C*, *CAT*, *cmlA*, *dfra1*, *dfra12*, *ermB*, *ermC*, *intI*, *mexC*, *mexE*, *qnr*, *repA, strA*, *strB*, *sul2*, *tetA*, *tetD, tetM, tetQ*, *tetW*, *tetX*, *tolC*, *vanA*, *vanC*, *vanH*, *vanT*, *vanW*, *vanX*, *vanY*, and *vanZ*. Seed sequences and Hidden Markov Models (HMMs) for each gene were downloaded from FunGene, and diverse protein and corresponding nucleotide sequences (reference sequences) were selected with gene-specific search parameters (**Table S1**). Briefly, minimum size amino acid was set to 70% of the HMM length; minimum HMM coverage was set to 80% as is recommended by Xander software for targeted gene assembly (Wang *et al.* 2015b); and a score cutoff was manually selected based on a notable score reduction between consecutive sequences, as suggested by the Ribosomal Database Project (personal communication). Reference sequences were de-replicated before being used in subsequent analysis, and final sequence numbers are included in **Table S1**.

Sample collection, sequencing, and quality control

Study site, soil sampling and soil biogeochemistry were all performed as described (Lee *et al.* 2017). Briefly, surface soils were sampled along a gradient of fire-impact that was determined from historical characterizations of the site (Elick 2011): fire-affected (n = 6), recovered (n = 5), and reference (n = 1). Fire-affected soils had elevated temperatures due to fire; recovered soils were at ambient temperature but historically had elevated temperatures from the fire; and the reference soil was never impacted by the fire. The reference sample was used as a qualitative control and is not intended as an quantitative and definitive comparison to non-impacted soils.

PeerJ Preprints | https://doi.org/10.7287/peerj.preprints.3484v1 | CC BY 4.0 Open Access | rec: 22 Dec 2017, publ: 22 Dec 2017

Microbial community DNA was obtained using a phenol chloroform extraction (Cho et al., 1996) and purification with MoBio DNEasy PowerSoil kit without vortexing. All samples were sequenced on the Illumina HiSeq 2500 platform with 2x150bp paired end format at the Joint Genome Institute (JGI) and quality filtered using BBDuk (https://sourceforge.net/projects/bbmap/). Metagenome coverage was estimated using Nonpareil (Rodriguez-R and Konstantinidis 2014).

Gene targeted assembly and quality control

A gene targeted metagenome assembler (Wang *et al.* 2015b) was used to assemble antibiotic resistance genes of interest from quality-filtered metagenomes. For each gene of interest, seed sequences, HMMs, and reference gene databases, as described above, were included. The *rplB* reference gene database, seed sequences, and HMMs from the Xander package were used. In most instances, default assembly parameters were used, except to incorporate differences in protein length (i.e. if the protein was shorter than default 150 aa, as was the case for *dfra1*, *dfra12*, *AAC6-Ia*, *ermB*, *ermC*, *qnr*, *vanX*, and *vanZ*) (**Table S1**). While the assembler includes chimera removal, additional quality control steps were added. Specifically, final assembled sequences (contigs) were searched against the reference gene database as well as the non-redundant database (nr) from NCBI (August 28, 2017) using BLAST (v. 2.2.26,(Camacho *et al.* 2008)). Genes were re-examined if the top hit had an e-value > 10^{-5} or if top hit descriptors were not the target gene. Genes with low quality results were re-assembled with adjusted parameters. Aligned sequences from each sample were dereplicated and clustered at 90, 97, and 99% amino acid identity using the RDP Classifier (Wang *et al.* 2007). Our quality control analyses can be accessed on GitHub ('assembly_assessments' repository in

PeerJ Preprints | https://doi.org/10.7287/peerj.preprints.3484v1 | CC BY 4.0 Open Access | rec: 22 Dec 2017, publ: 22 Dec 2017

https://github.com/ShadeLab/PAPER_Dunivin_Antibiotics_2017/tree/master/assembly_assessments).

Ecological analyses

Phylum-level *rplB* relative abundance was used to examine differences in community structure. Relative abundance for each site was averaged among samples of the same fire classification (i.e. fire-affected, recovered, reference) and compared to 16S rRNA gene sequence data from a previous work (Lee *et al.* 2017). For subsequent ecological analyses, the RDP Classifier was used to generate an OTU table from 90, 97, and 99% amino acid identities. We refer to contigs clustered at 99% identity as "ARG sequences" throughout the remainder of the text. The OTU tables were analyzed in R (R Development Core Team 2008). OTU tables were separated based on the gene of interest (*rplB* and ARGs). Due to Nonpareil-estimated differences in coverage, OTU tables were rarefied to an even sampling depth (258 and 180 assembled sequences respectively) using the vegan package (Oksanen *et al.* 2017). Pieluo's evenness was calculated, and richness was estimated using PhyloSeq (McMurdie and Holmes 2013). The Psych package was used to calculate Spearman's rank correlations between alpha diversity (richness and evenness) and soil temperature for both *rplB* and ARGs. Bray-Curtis distance was used to obtain dissimilarity matrices, and principal component analysis was used to visualize beta diversity. Distance matrices of rarefied, relativized data were analyzed using Mantel tests with Spearman's rank correlations. Mantel tests were performed on *rplB*, ARG, and spatial distance matrices of sample locations.

Resistance gene comparison

PeerJ Preprints | https://doi.org/10.7287/peerj.preprints.3484v1 | CC BY 4.0 Open Access | rec: 22 Dec 2017, publ: 22 Dec 2017

We assessed ARG biogeography at the gene, taxonomic class, and sequence levels. To compare the abundance of ARGs among data sets, total counts of *rplB* were used to normalize the abundance of each ARG sequence. Total counts of each ARG were calculated as the sum of the relative abundance of each ARG sequence. The Psych package (Revelle 2017) was used to calculate Spearman's rank correlations between soil geochemical properties and total gene counts for each ARG. Pairwise correlations for the total abundance of each resistance gene were also calculated. For taxonomic analysis of each ARG, the top BLAST result and the taxize package (Chamberlain *et al.* 2017) were used to assign taxonomy to each ARG sequence. When the top hit was an uncultured bacterium, the second or third hit was used, and when all three top hits were unknown, the taxonomy was labeled unknown. Total counts of each taxonomic class were summed for each ARG, and Spearman's rank correlations were used to test for correlations between class abundance and temperature for all ARGs with representatives from at least three taxanomic groups. Spearman's rank correlations were performed on normalized and relativized abundance information, but only relativized abundance is shown because it agreed with normalized data and also had unique features. Furthermore, we examined individual ARG sequence dynamics. A Venn analysis was performed between ARGs in fire affected and recovered samples using the VennDiagram package (Chen and Boutros 2011). The mean normalized abundance for each ARG sequence among samples was plotted against the number of sites it was observed in (occurrence). ARG sequences present in only one site were subsequently removed, and we used hierarchical cluster analysis with the stats package to examine similar sequence dynamics along the temperature gradient. Relative abundance of each resulting cluster was plotted against temperature.

PeerJ Preprints | https://doi.org/10.7287/peerj.preprints.3484v1 | CC BY 4.0 Open Access | rec: 22 Dec 2017, publ: 22 Dec 2017

208 *Reproducibility, code, and data*

209 Our computing workflows and R script can be accessed on GitHub

210 (https://github.com/ShadeLab/PAPER_Dunivin_Antibiotics_2017). Metagenomes are available

211 from IMG/GOLD study ID: Gs0114513.

212

213

214 **Results and Discussion**

215 *Soil samples and gene targeted assembly*

216 We previously collected soils along the Centralia temperature gradient (Lee *et al.* 2017).

217 We submitted DNA extracted from twelve soils (temperature range = 12.1-54.2°C) to the Joint

218 Genome Institute for small-scale Community Science Project; we did not submit all 18 originally

219 collected samples because there was a 12-sample limit with the small-scale award, and so we

220 chose samples for sequencing that were representative of the thermal gradient. We sequenced

221 metagenomes from soils that had elevated temperatures due to the fire (fire-affected, n = 6),

222 those that were historically impacted (recovered, n = 5), and those with no documented impact

223 (reference, n = 1) (**Figure S1**). Quality filtered metagenome size ranged from 21-51 Gbp, and

224 Nonpareil-estimated coverage (Rodriguez-R and Konstantinidis 2014) varied from 29.12 to

225 89.96% (**Table S2**). Though we measured a suite of geochemical data (**Table S3**), our previous

226 work found temperature to be the strongest driver of community structure (Lee *et al.* 2017); we

227 found that ARGs only correlated with temperature (**Table S4**).

228 We used a gene-targeted metagenome assembler to probe Centralia metagenomes for

229 ARGs. While this gene-centric methodology does not permit analysis of entire gene cassettes or

230 flanking regions, it improves detection of low abundance genes, increases the length of

PeerJ Preprints | https://doi.org/10.7287/peerj.preprints.3484v1 | CC BY 4.0 Open Access | rec: 22 Dec 2017, publ: 22 Dec 2017

assembled gene sequences, and is capable of detecting strain-level sequence variation (Wang *et al.* 2015b). In addition to assembling ARGs of interest, we assembled *rplB*, a single copy gene and phylogenetic marker. We found that *rplB* assembled using these methods was comparable 16S rRNA gene data (**Supplementary results**; **Figure S2**), showing that gene targeted assembly produced results consistent with previous work.

Detected ARGs and changes in their abundance with temperature

We examined a suite of genes encoding resistance to aminoglycosides, beta-lactams, chloramphenicol, sulfonamides, tetracyclines, trimethoprim, and vancomycin, as well as plasmid-related and genes encoding multidrug efflux pumps (**Table 1**). From Centralia metagenomes, we assembled 1,165 unique ARG clustered at 99% amino acid identity. Though we targeted 35 distinct types of ARGs and two HGT-related genes, only 17 of these could be assembled from Centralia metagenomes. The genes *ANT3*, *ANT6*, *ANT9*, CAT, *dfra1*, *ermB*, *ermC*, *mexC*, *mexE*, *qnr*, *repA*, *strA*, *strB*, *tetD*, *tetM*, *tetQ*, *vanC*, *vanT*, *vanW*, and *vanY* were not observed, suggesting that they were either below detection or absent. For detected ARGs, we found positive correlations between *vanA, H, and X* genes and between *tolC* and *dfra12* (**Figure S3**). *vanAHX* genes are known to be associated with one another in VanA-type operons (Périchon and Courvalin 2009), and genes *tolC* and *dfra12* have previously been observed in isolates (Wannaprasat, Padungtod and Chuanchuen 2011). While *sul2* and *intI1* have been previously shown to be correlated (Johnson *et al.* 2016), we did not observe a significant correlation between these genes. This discrepancy could be because our analysis does not distinguish between integron classes. Several ARGs in Centralia were negatively correlated with soil temperature (**Figure 1; Table S4**), but no ARGs were correlated with other measured soil

PeerJ Preprints | https://doi.org/10.7287/peerj.preprints.3484v1 | CC BY 4.0 Open Access | rec: 22 Dec 2017, publ: 22 Dec 2017

geochemical properties (results not shown, **Table S3**). The most abundant ARGs detected in Centralia were *adeB*, *bla_B*, and *dfra12* (**Figure 1, Figure S4**). We note that the highest ARG normalized abundance was typically in Cen04 (13.3°C) but that this is due to low *rplB* abundance in the sample.

Our results are generally in agreement with other studies of ARGs in soils. For example, Fitzpatrick and Walsh 2016 also reported low abundance or absence of *qnr*, *tet* and *van* genes in soil. Several studies also reported that genes encoding dihydrofolate reductases and/or beta-lactamases were abundant in soils (Forsberg *et al.* 2014; Fitzpatrick and Walsh 2016; Li, Xia and Zhang 2017). Previous studies reported reductions in clinically-relevant ARGs with increased temperatures in digesters and compost (Diehl and Lapara 2010; Qian *et al.* 2016; Tian *et al.* 2016). Diehl and Lapara (2010) observed a negative relationship between temperature and genes encoding tetracycline resistance and class 1 integrons in anaerobic digesters, but not aerobic ones. This may be further relevant to Centralia soils, as there likely are pockets of anaerobic activity in hot soils, especially at venting sites, which have measurably higher percent moisture content due to steam escaping (**Table S3**). To our knowledge, this is the first description of a reduction in ARG abundances with temperature *in situ* with soil. These results suggest that ARGs may be reduced in soil environments by increasing temperature. Thus, we speculate that increases in temperatures expected to reduce microbial community diversity may result in decreased clinically relevant ARGs in the environment.

Diversity of ARGs

We also examined the amino acid-level diversity of ARGs in Centralia metagenomes. We tested sequence cutoffs of 90, 97, and 99% amino acid identity, but overarching patterns did

PeerJ Preprints | https://doi.org/10.7287/peerj.preprints.3484v1 | CC BY 4.0 Open Access | rec: 22 Dec 2017, publ: 22 Dec 2017

not vary based on sequence cutoff (results not shown). Thus, our subsequent diversity analysis applied the most stringent cutoff (99% amino acid identity), as was applied in the original gene targeted assembly paper (Wang *et al.* 2015b). ARG richness was negatively correlated with temperature ($\rho = -0.57$; $p < 0.05$), but evenness had a variable response with temperature ($\rho = -0.47$; $p > 0.05$) (**Figure 2BD**). ARG alpha diversity (within-sample) trends were thus similar to *rplB* and 16S rRNA gene diversity trends (**Supplementary results**; **Figure 2AC**), highlighting the influence of community structure on soil ARG profiles. In addition, overall differences in the composition of ARGs among sites were related to differences in *rplB* community structure (Mantel's $r = 0.54$; $p < 0.05$ on 999 permutations; **Figure S5**). This result also supports that compositional shifts in membership among Centralia sites were driving the observed differences in ARGs, not propagation of ARGs by gene transfer. These results agree with a recent analysis that reported congruence between community structure and ARG profiles in soils (Forsberg *et al.* 2014). Similar to patterns in *rplB* and 16S rRNA genes, ARG profiles could not be explained by distance between sample sites (Mantel's $r = 0.01$, $p > 0.05$ on 999 permutations). This suggests that local dispersal of ARGs, which could be indicative of HGT, is not a common mechanism of ARG dissemination in this system. However, when we considered fire-affected and recovered metagenomes separately, we found that *rplB* community structure explained ARG composition in fire-affected soils (Mantel's $r = 0.71$; $p < 0.05$ on 719 permutations), but not in recovered soils (Mantel's $r = 0.30$; $p > 0.05$ on 119 permutations). We determined that this result was not driven by one anomalous sample by performing iterative "leave-one-out" Mantel tests with four of five recovered soils, and all tests showed no correlation between *rplB* and ARGs (results not shown). The reason for no relationship between *rplB* and ARG in recovered soils is unclear (one hypothesis is that there is no signal given higher diversity), but this observation very indirectly

PeerJ Preprints | https://doi.org/10.7287/peerj.preprints.3484v1 | CC BY 4.0 Open Access | rec: 22 Dec 2017, publ: 22 Dec 2017

suggests a potential larger influence of HGT in recovered soils than fire-affected soils that could be explored in future work.

ARG distribution and sequence-specific biogeography

Only twelve ARG sequences were shared between fire-affected and recovered soils (**Figure 3A**). On one hand, this is expected because soils are heterogeneous and have high ARG diversity (Fitzpatrick and Walsh 2016). Forsberg and colleagues (2014) observed 2,895 ARG sequences in a functional antibiotic resistance screen from 18 agricultural and grassland soils. Of these, only 2.6% were present in two or more soils, which is comparable to our data (1.1%). Similarly, the distinction between fire-affected and recovered soil in our study is in part explained by generally high ARG diversity, with minimal overlap of ARG sequences detected between all sites. Furthermore, most ARG sequences (94.16%), whether they were rare (< 1.5% normalized abundance to *rplB*) or prevalent, were detected only in one metagenome (**Figure 3B**). Though the gene-targeted assembly approach maximizes observation of diversity given metagenome coverage, it is possible that even greater coverage of these metagenomes could result in detection of more shared ARG sequences between samples. There were 13 distinct biogeographical dynamics that indicated genes sensitive to the fire, and these were classified into two categories based on their prevalence and patterns of detection: abundant-transient, and rare-transient sequences (**Figure 4**). Abundant-transient ARG sequences belonged to genes *adeB*, *bla_B*, *dfra12*, *intI*, *sul2*, and *vanZ*. These sequences had a *rplB*-normalized abundance of ≥ 1.5% of the total community within at least one metagenome. Rare-transient biogeographic patterns were observed for ARG sequences belonging to *adeB*, *bla_A*, *bla_B*, CEP, *dfra12*, *intI*, *tolC*, *vanA*, *vanX*, and *vanH*. Rare-transient sequences represented those with ≤ 1.5% of the total

PeerJ Preprints | https://doi.org/10.7287/peerj.preprints.3484v1 | CC BY 4.0 Open Access | rec: 22 Dec 2017, publ: 22 Dec 2017

community. However, step-wise relationships with temperature were observed for several ARG sequences, suggesting the potential enrichment by fire for microbes harboring these ARG sequences. Two clusters of rare-transient sequences with no temperature relationship were observed based on differences in normalized abundance (**Figure 4**), suggesting that they had no relationship with fire or temperature. Thus, we observed sequence-specific biogeography for ARG sequences along the temperature gradient, showing that the average changes in ARG abundance does not always fully explain the dynamics of each unique resistance gene sequence detected within that gene family.

ARG Compositional shifts

We examined both *rplB*-normalized and relativized abundance patterns to compare changes in composition of ARGs and changes in proportional contributions of ARGs. For this analysis, composition was considered at the phylum or *Proteobacteria* class levels based on top BLAST hits. For ARGs that represented more than three phyla or *Proteobacteria* classes, (*bla_A*, *bla_B*, *dfra12*, *intI*) (**Table S5; Table S6**), we explored for correlations with temperature. We observed changes in ARG composition with temperature for *bla_A*, *dfra12*, and *intI* (**Figure 5**).

Generally, community structure was associated with ARG composition. *rplB*-level reduction in *Betaproteobacteria* corresponded with reductions in *Betaproteobacteria*-related ARG. *Betaproteobacteria*-related *bla_A* and *dfra12* genes decreased with temperature (**Figure 5**; **Table S6**). Thus, reductions in total *bla_A* and *dfra12* counts is largely explained by a reduction in *Betaproteobacteria*. This pattern does not extend to *bla_B* since *Betaproteobacteria*-related *bla_B* genes were only detected in one soil (Cen16). We did not detect changes in *Gammaproteobacteria* based on *rplB*. This corresponded with consistent relative abundances of

PeerJ Preprints | https://doi.org/10.7287/peerj.preprints.3484v1 | CC BY 4.0 Open Access | rec: 22 Dec 2017, publ: 22 Dec 2017

346 *Gammaproteobacteria*-related *bla_A*, *bla_B*, *dfra12*, and *intI* (**Table S6**).
347 *Gammaproteobacteria*-related *dfra12* increased in relative abundance with soil temperature (ρ =
348 0.95, $p < 0.05$), further highlighting that a reduction in total *dfra12* relative abundance is not due
349 to changes in *Gammaproteobacteria*-related sequences. Phylum-level community structure,
350 therefore, corresponded with compositional changes in ARGs, highlighting the influence of the
351 underlying community on soil ARGs.
352 We observed evidence for functional redundancy of ARGs in Centralia through
353 compositional shifts along the temperature gradient. Total *bla_A* relative abundance decreased
354 with temperature (**Figure 1**); however, taxonomic groups of *bla_A* were differentially impacted
355 along the temperature gradient (**Figure 5**; **Table S6**). Both normalized and relativized abundance
356 of *Actinobacteria*-related *bla_A* genes increased ($\rho > 0.6$, $p < 0.05$) while *Betaproteobacteria*-
357 related *bla_A* genes decreased ($\rho < 0.6$, $p < 0.05$) with temperature (**Table S6**). Thus, fire
358 impacted the abundance and composition of *bla_A*. A decrease in total *bla_A* (**Figure 1**) was
359 accompanied by an increase in *Actinobacteria*-related *bla_A* This asymmetric response with
360 temperature suggests an impact of functional redundancy on soil ARG profiles. We also
361 observed a shift in *intI* composition despite consistent *intI* abundance along the temperature
362 gradient. The relative abundance of *Beta*- and *Gammaproteobacteria*-related *intI* decreased with
363 temperature ($\rho < 0.6$, $p < 0.05$), but the relative abundance of *Nitrospirae*-related *intI* increased
364 with temperature ($\rho > 0.6$, $p < 0.05$) (**Figure 5**; **Table S6**). We therefore observed changes in
365 composition of *intI* with fire despite a lack of change in total *intI* abundance. Notably, previous
366 studies have described *Nitrospirae*-related *intI*. Oliveira-Pinto and colleagues (2016) isolated an
367 *intI* gene cassette related to *Nitrospirae* from a metal-rich stream, and Goltsman and colleagues
368 (2009) identified both integrase and ARGs on chromosomes of *Nitrospirae* strains isolated from

PeerJ Preprints | https://doi.org/10.7287/peerj.preprints.3484v1 | CC BY 4.0 Open Access | rec: 22 Dec 2017, publ: 22 Dec 2017

acid mine drainage. It is unclear, however, whether *Nitrospirae*-related *intI* genes are associated with ARG transfer. As *intI* encodes for a DNA integrase, this result suggests that *Nitrospirae* might contribute more to HGT in fire affected soils, but we cannot determine whether this putative gene transfer would include ARGs. We posit that reductions in ARG abundance due to increased temperature could increase subsets of clinically relevant ARGs, and studies using temperature as a control for ARGs should consider sequence-level ARG dynamics within the system.

Conclusions

This case study of ARG biogeography over a long-term, severe thermal disturbance demonstrates the importance of community structure on soil ARG abundance and composition. Despite the stressor and the withdrawal of human activity, the diversity of ARG observed in Centralia is comparable to other soil systems (Forsberg *et al.* 2014; Fitzpatrick and Walsh 2016). For several clinically relevant ARGs, we observed a reduction in total abundance with increased temperature. While this has been reported in anthropogenic systems (Diehl and Lapara 2010; Qian *et al.* 2016; Tian *et al.* 2016), we further probed Centralia datasets for compositional and sequence-specific ARG dynamics and found nuanced results. Generally, the reduction in ARG abundance could be explained by indirect effects (i.e. compositional shifts in the community). We posit that increased temperatures could result in a reduction in the diversity and abundance of ARGs in the environment, but our data also suggest that this reduction will not impact all ARG sequences similarly. ARG biogeographical dynamics in soil are thus largely dependent on community structure, which may also drive observed fine-scale abundance-occurrence patterns.

PeerJ Preprints | https://doi.org/10.7287/peerj.preprints.3484v1 | CC BY 4.0 Open Access | rec: 22 Dec 2017, publ: 22 Dec 2017

Acknowledgements

This research was supported through computational resources provided by the Institute for Cyber-Enabled Research. We thank the Ribosomal Database Project for their advice on reference gene database construction. We thank Trevor Grady for graphic design assistance in creating Figure S1.

Conflict of Interest

The authors declare no conflicts of interest.

Funding

Metagenome sequencing was supported by the Joint Genome Institute Community Science Project #1834. The work conducted by the U.S. Department of Energy Joint Genome Institute, a DOE Office of Science User Facility, is supported under Contract No. DE-AC02-05CH11231. TKD was supported by the Department of Microbiology and Molecular Genetics Ronald and Sharon Rogowski Fellowship for Food Safety and Toxicology Graduate Fellowship.

References

Allen HK, Donato J, Wang HH *et al.* Call of the wild: antibiotic resistance genes in natural environments. *Nat Rev Microbiol* 2010;**8**:251–9.

Aminov RI, Mackie RI. Evolution and ecology of antibiotic resistance genes. *FEMS Microbiol Lett* 2007;**271**:147–61.

Berendonk TU, Manaia CM, Merlin C *et al.* Tackling antibiotic resistance: the environmental framework. *Nat Rev Microbiol* 2015;**13**:310–7.

PeerJ Preprints | https://doi.org/10.7287/peerj.preprints.3484v1 | CC BY 4.0 Open Access | rec: 22 Dec 2017, publ: 22 Dec 2017

415 Camacho C, Coulouris G, Avagyan V *et al.* BLAST+: architecture and applications. *BMC*
416 *Bioinformatics* 2008;**10**.
417 Chamberlain S, Szoecs E, Foster Z *et al.* Taxanomic information from around the web. 2017.
418 Chen H, Boutros PC. VennDiagram: A package for the generation of highly-customizable Venn
419 and Euler diagrams in R. *BMC Bioinformatics* 2011;**12**, DOI: 10.1186/1471-2105-12-35.
420 Diehl DL, Lapara TM. Effect of temperature on the fate of genes encoding TC resistance and the
421 integrase of class 1 integrons within anaerobic and aerobic digesers treating municipal
422 wastewater solids.pdf. *Environ Sci Technol* 2010;**44**:9128–33.
423 Elick JM. Mapping the coal fire at Centralia, Pa using thermal infrared imagery. *Int J Coal Geol*
424 2011;**87**:197–203.
425 Fierer N, Leff JW, Adams BJ *et al.* Cross-biome metagenomic analyses of soil microbial
426 communities and their functional attributes. *Proc Natl Acad Sci* 2012;**109**:21390–5.
427 Fish JA, Chai B, Wang Q *et al.* FunGene: The functional gene pipeline and repository. *Front*
428 *Microbiol* 2013, DOI: 10.3389/fmicb.2013.00291.
429 Fitzpatrick D, Walsh F. Antibiotic resistance genes across a wide variety of metagenomes. *FEMS*
430 *Microbiol Ecol* 2016;**92**:1–8.
431 Forsberg KJ, Patel S, Gibson MK *et al.* Bacterial phylogeny structures soil resistomes across
432 habitats. *Nature* 2014;**509**:612–6.
433 Garner E, Wallace JS, Argoty GA *et al.* Metagenomic profiling of historic Colorado Front Range
434 flood impact on distribution of riverine antibiotic resistance genes. *Sci Rep* 2016;**6**:38432.
435 Gibson MK, Forsberg KJ, Dantas G. Improved annotation of antibiotic resistance determinants
436 reveals microbial resistomes cluster by ecology. *ISME J* 2014;**9**:1–10.
437 Goltsman DSA, Denef VJ, Singer SW *et al.* Community genomic and proteomic analyses of

PeerJ Preprints | https://doi.org/10.7287/peerj.preprints.3484v1 | CC BY 4.0 Open Access | rec: 22 Dec 2017, publ: 22 Dec 2017

chemoautotrophic iron-oxidizing "Leptospirillum rubarum" (Group II) and "Leptospirillum ferrodiazotrophum" (Group III) bacteria in acid mine drainage biofilms. *Appl Environ Microbiol* 2009;**75**:4599–615.

Hiltunen T, Virta M, Laine A-L. Antibiotic resistance in the wild : an eco- evolutionary perspective. *Philos Trans R Soc B* 2017;**372**.

Van Hoek AHAM, Mevius D, Guerra B *et al.* Acquired antibiotic resistance genes: An overview. *Front Microbiol* 2011;**2**:1–27.

Janzen C, Tobin-Janzen T. Microbial Communities in Fire-Affected Soils. In: Dion P, Nautiyal CS (eds.). *Microbiology of Extreme Soils*. Springer Berlin Heidelberg, 2008, 299–316.

Johnson TA, Stedtfeld RD, Wang Q *et al.* Clusters of antibiotic resistance genes enriched together stay together in swine agriculture. *MBio* 2016, DOI: 10.1128/mBio.02214-15.

Kahn LH. *One Health Initiative: Antimicrobial Resistance in the Environment*., 2016.

Kumar K, C. Gupta S, Chander Y *et al.* Antibiotic Use in Agriculture and Its Impact on the Terrestrial Environment. *Advances in Agronomy*. Vol 87. 2005, 1–54.

Laine A-L, Hiltunen T, Virta M. Antibiotic resistance in the wild: an eco- evolutionary perspective. *Philos Trans R Soc B Biol Sci* 2016;**372**, DOI: 10.1098/rstb.2016.0039.

Lang KS, Anderson JM, Schwarz S *et al.* Novel florfenicol and chloramphenicol resistance gene discovered in alaskan soil by using functional metagenomics. *Appl Environ Microbiol* 2010;**76**:5321–6.

Lee S-H, Sorensen JW, Grady KL *et al.* Divergent extremes but convergent recovery of bacterial and archaeal soil communities to an ongoing subterranean coal mine fire. *ISME J* 2017, DOI: 10.1038/ismej.2017.1.

Li L-G, Xia Y, Zhang T. Co-occurrence of antibiotic and metal resistance genes revealed in

PeerJ Preprints | https://doi.org/10.7287/peerj.preprints.3484v1 | CC BY 4.0 Open Access | rec: 22 Dec 2017, publ: 22 Dec 2017

complete genome collection. *ISME J* 2017;**11**:651–62.

McMurdie PJ, Holmes S. Phyloseq: An R Package for Reproducible Interactive Analysis and Graphics of Microbiome Census Data. *PLoS One* 2013;**8**, DOI: 10.1371/journal.pone.0061217.

Melody SM, Johnston FH. Coal mine fires and human health: What do we know? *Int J Coal Geol* 2015;**152**, **Part**:1–14.

Nesme J, Simonet P. The soil resistome: A critical review on antibiotic resistance origins, ecology and dissemination potential in telluric bacteria. *Environ Microbiol* 2015;**17**:913–30.

Nunes I, Jacquiod S, Brejnrod A *et al.* Coping with copper : legacy effect of copper on potential activity of soil bacteria following a century of exposure. *FEMS Microbiol Ecol* 2016;**92**, DOI: 10.1093/femsec/fiw175.

Oksanen J, Guillaume Blanchet F, Friendly M *et al.* Community Ecology Package, Package " vegan ." 2017, DOI: ISBN 0-387-95457-0.

Oliveira-Pinto C, Costa PS, Reis MP *et al.* Diversity of gene cassettes and the abundance of the class 1 integron-integrase gene in sediment polluted by metals. *Extremophiles* 2016;**20**:283–9.

Pal C, Bengtsson-Palme J, Kristiansson E *et al.* Co-occurrence of resistance genes to antibiotics, biocides and metals reveals novel insights into their co-selection potential. *BMC Genomics* 2015, DOI: 10.1186/s12864-015-2153-5.

Périchon B, Courvalin P. VanA-type vancomycin-resistant Staphylococcus aureus. *Antimicrob Agents Chemother* 2009;**53**:4580–7.

Qian X, Sun W, Gu J *et al.* Reducing antibiotic resistance genes, integrons, and pathogens in dairy manure by continuous thermophilic composting. *Bioresour Technol* 2016;**220**:425–32.

PeerJ Preprints | https://doi.org/10.7287/peerj.preprints.3484v1 | CC BY 4.0 Open Access | rec: 22 Dec 2017, publ: 22 Dec 2017

484 R Development Core Team. R: A language and environment for statistical computing. 2008.
485 Revelle W. Procedures for Psychological, Psychometric, and Personality Research. 2017.
486 Rizzo L, Manaia C, Merlin C *et al.* Urban wastewater treatment plants as hotspots for antibiotic
487 resistant bacteria and genes spread into the environment: A review. *Sci Total Environ*
488 2013;**447**:345–60.
489 Rodriguez-R LM, Konstantinidis KT. Nonpareil: A redundancy-based approach to assess the
490 level of coverage in metagenomic datasets. *Bioinformatics* 2014, DOI:
491 10.1093/bioinformatics/btt584.
492 Shade A, Peter H, Allison SD *et al.* Fundamentals of microbial community resistance and
493 resilience. *Front Microbiol* 2012;**3**:1–19.
494 Tian Z, Zhang Y, Yu B *et al.* Changes of resistome, mobilome and potential hosts of antibiotic
495 resistance genes during the transformation of anaerobic digestion from mesophilic to
496 thermophilic. *Water Res* 2016;**98**:261–9.
497 Wang FH, Qiao M, Chen Z *et al.* Antibiotic resistance genes in manure-amended soil and
498 vegetables at harvest. *J Hazard Mater* 2015a;**299**:215–21.
499 Wang Q, Fish JA, Gilman M *et al.* Xander : employing a novel method for efficient gene-
500 targeted metagenomic assembly. *Microbiome* 2015b;**3**:32.
501 Wang Q, Garrity GM, Tiedje JM *et al.* Naive Bayesian classifier for rapid assignment of rRNA
502 sequences into the new bacterial taxonomy. *Appl Environ Microbiol* 2007;**73**.
503 Wannaprasat W, Padungtod P, Chuanchuen R. Class 1 integrons and virulence genes in
504 Salmonella enterica isolates from pork and humans. *Int J Antimicrob Agents* 2011;**37**:457–
505 61.
506

PeerJ Preprints | https://doi.org/10.7287/peerj.preprints.3484v1 | CC BY 4.0 Open Access | rec: 22 Dec 2017, publ: 22 Dec 2017

Table 1. Resistance genes tested in this study.

Antibiotic specificity	Gene
Aminoglycoside	AAC6-Ia, ANT3, ANT6, ANT9, strA,B
β-Lactams	Class A (bla_A), Class B (bla_B), Class C (bla_C)
Chloramphenicol	CAT, cmlA
Macrolide	ermB,C, qnr
Multidrug efflux	adeB, mexC,E, tolC
Plasmid	intI, repA
Sulfonamide	sul2
Tetracycline	tetA,D,M,Q,W,X
Trimethoprim	dfra1, dfra12
Vancomycin	vanA,C,H,T,W,X,Y,Z

Figure 1. Negative correlations between normalized abundance of ARGs and soil temperature. Coverage-adjusted abundance for *bla_A*, *bla_B*, *tolC*, and *dfra12* was normalized to total abundance of the single copy gene *rplB*. Normalized abundance is plotted against soil temperature. Note the differences in y-axes. The linear trend line and p value corresponding to the Spearman's rank correlation are shown. Shape indicates soil classification based on fire history.

Figure 2. Observed richness (AB) and evenness (CD) of *rplB* (AC) and ARG (BD) along the Centralia temperature gradient. Assembled sequences were clustered at 99% amino acid identity and rarefied to an even sampling depth. Observed number of sequences (richness) and Pielou's evenness is plotted against soil temperature. Shape indicates soil classification based on fire history.

Figure 3. Presence of ARG sequences in Centralia metagenomes. (A) Venn diagram of ARG sequences observed in recovered and fire-affected soils. **(B)** ARG abundance-occurrence patterns in Centralia metagenomes. Percent normalized abundance of ARG sequences was averaged among 12 metagenomes and plotted against the number of sites each sequence occurs in. Each point represents one cluster, and color indicates gene.

Figure 4. Normalized abundance of ARG sequences in Centralia metagenomes. Abundance of each gene sequence (clustered at 99% amino acid identity) present in ≥2 metagenomes was normalized to *rplB*. Complete-linkage clustering was calculated with the *rplB*-normalized abundance of each ARG sequence. Heatmap shows normalized abundance on a blue scale. Soil sites (column) are ordered by increasing soil temperature. Each row represents one ARG sequence, and ARG is noted by color.

Figure 5. Relative abundance of taxonomically similar ARGs. Phylum-level taxonomy for *bla_A*, *bla_B*, *dfra12*, *intI*, and *rplB* for each site is shown. Color indicates phylum- and *Proteobacteria* class-level taxonomy of ARGs, and sites are ordered by increasing soil temperature. *dfra12* was not detected in Cen01.

Figure 1

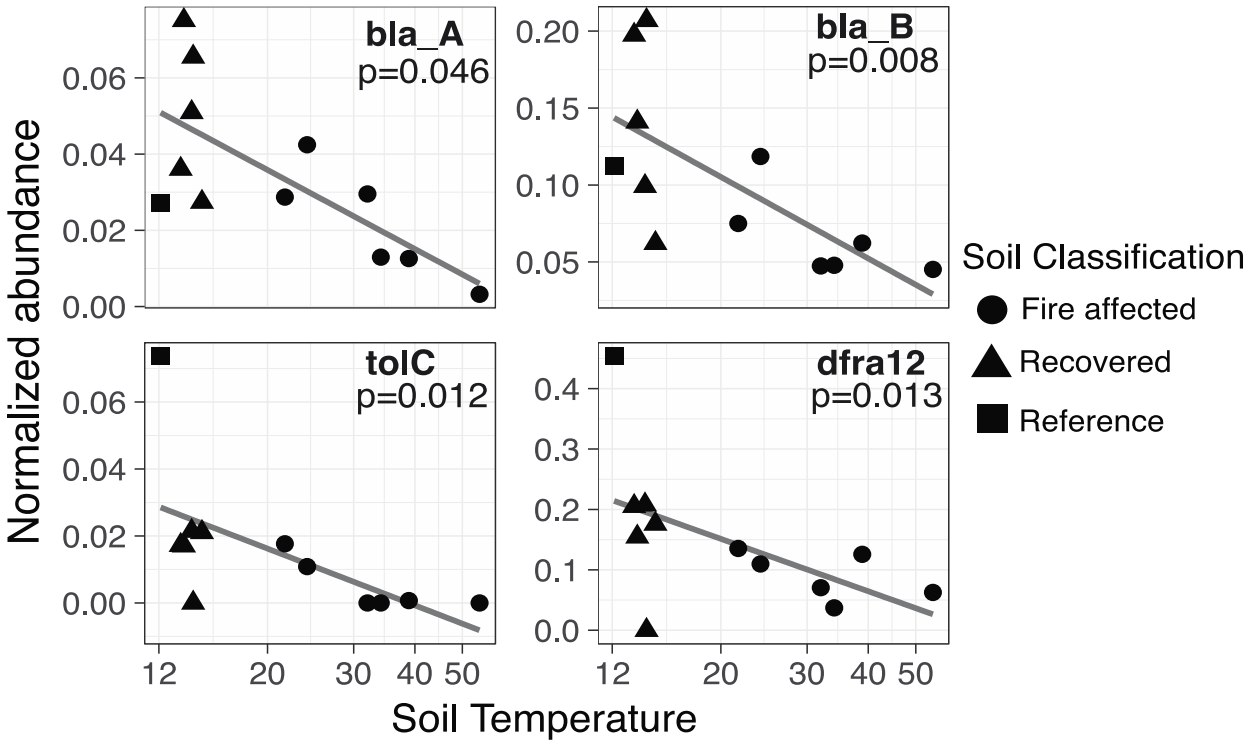

Figure 2

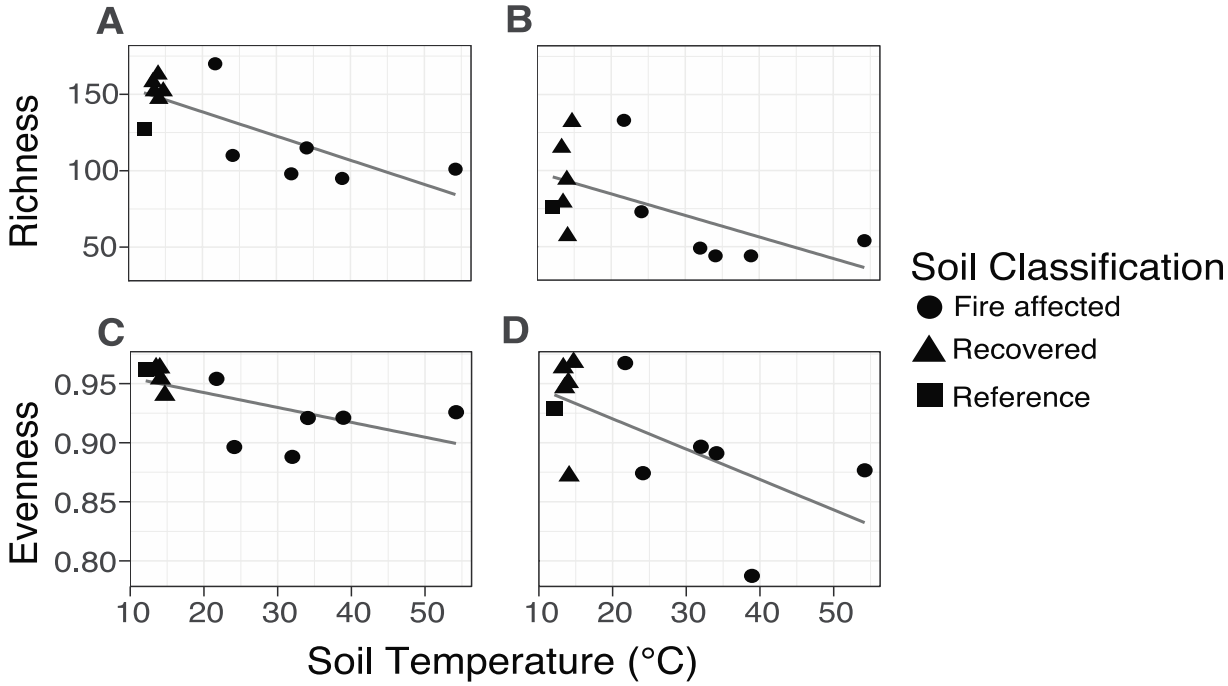
A
B
C
D
Richness
Evenness
150
100
50
0.95
0.90
0.85
0.80
10
20
30
40
50
Soil Temperature (°C)
Soil Classification
Fire affected
Recovered
Reference

Figure 3

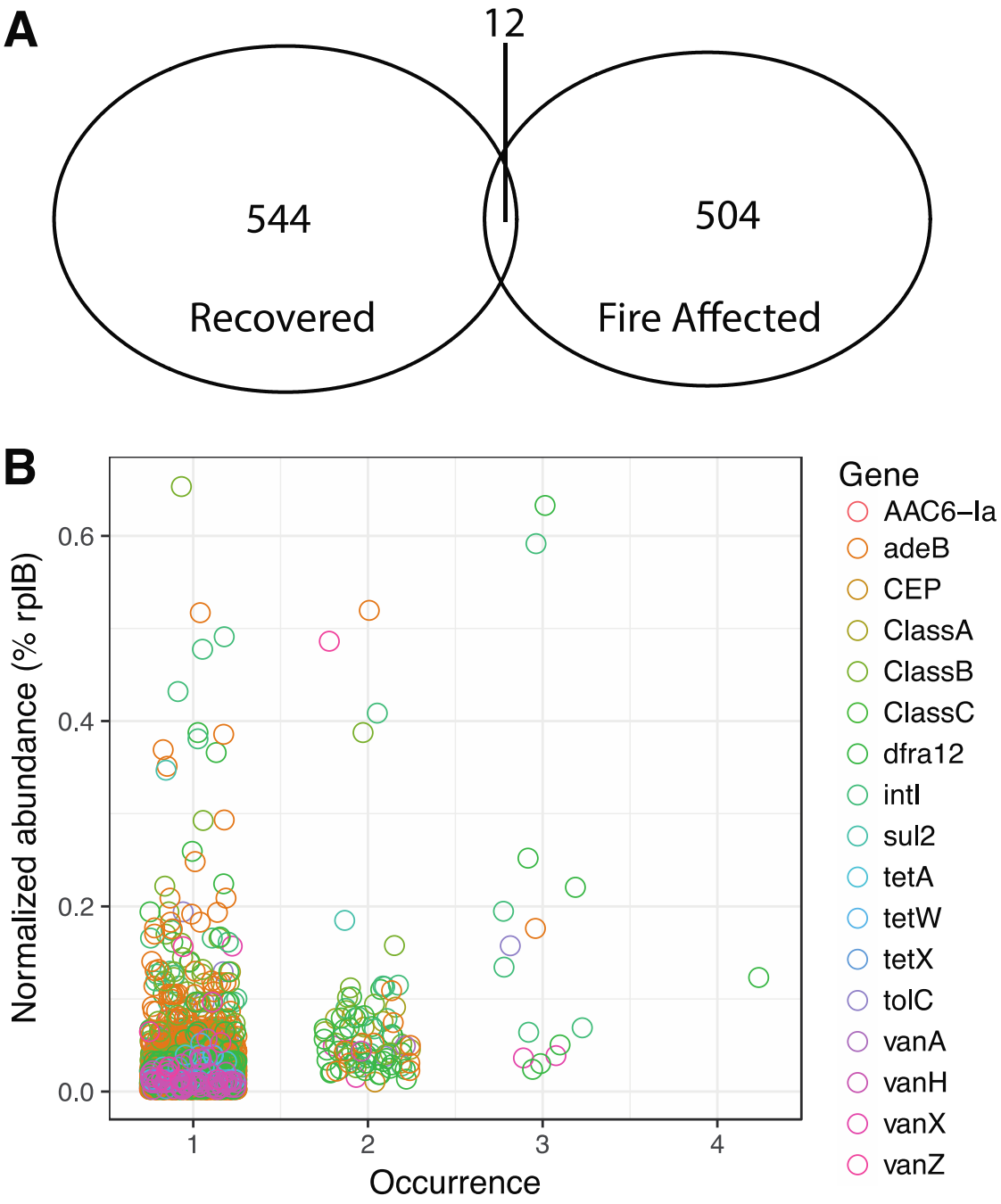
A
12
544
Recovered
504
Fire Affected
B
Normalized abundance (% rplB)
0.0
0.2
0.4
0.6
1
2
3
4
Occurrence
Gene
AAC6–Ia
adeB
CEP
ClassA
ClassB
ClassC
dfra12
intI
sul2
tetA
tetW
tetX
tolC
vanA
vanH
vanX
vanZ

Figure 4

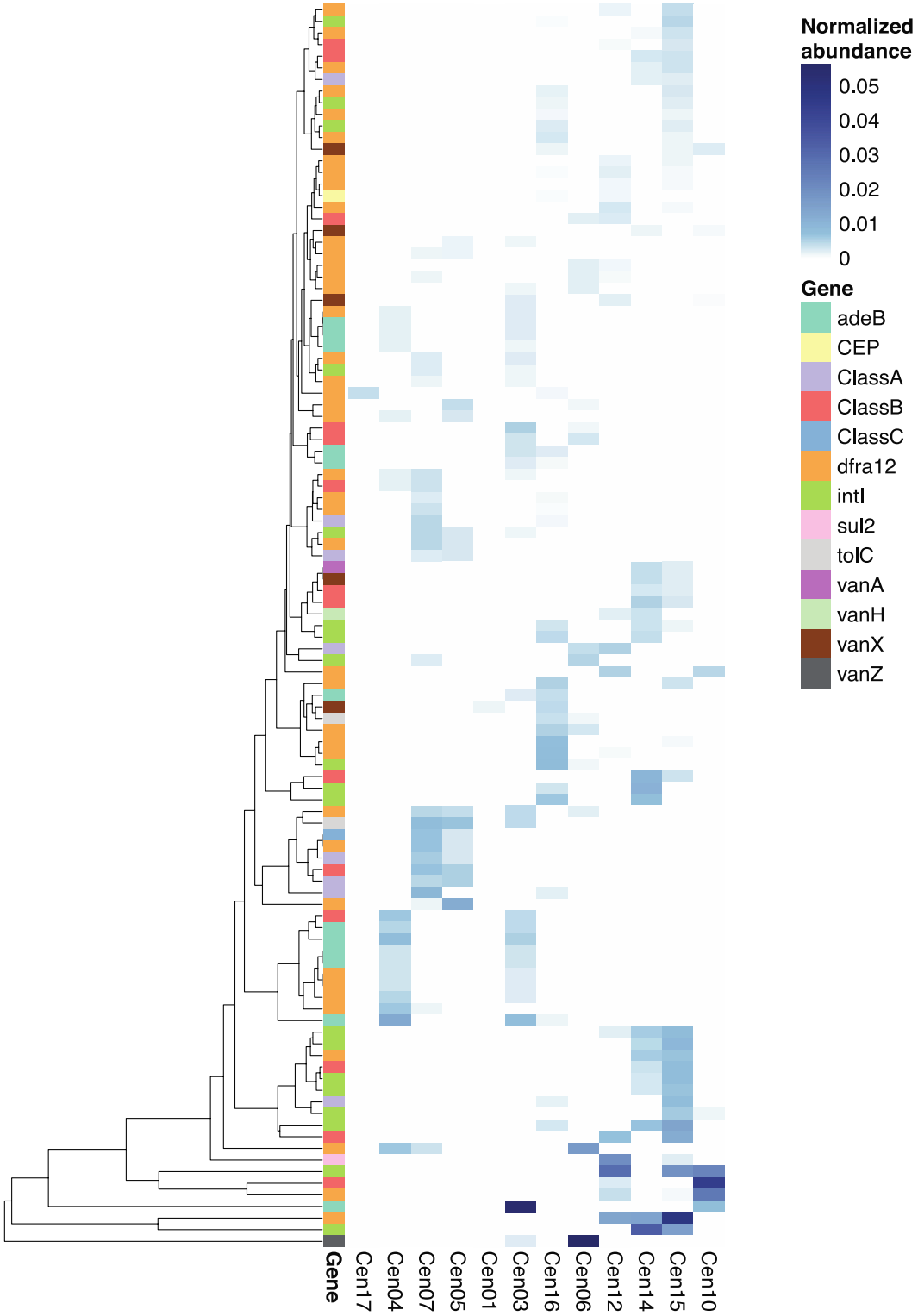
Normalized abundance
0.05
0.04
0.03
0.02
0.01
0
Gene
adeB
CEP
ClassA
ClassB
ClassC
dfra12
intI
sul2
tolC
vanA
vanH
vanX
vanZ
Gene
Cen17
Cen04
Cen07
Cen05
Cen01
Cen03
Cen16
Cen06
Cen12
Cen14
Cen15
Cen10

Figure 5

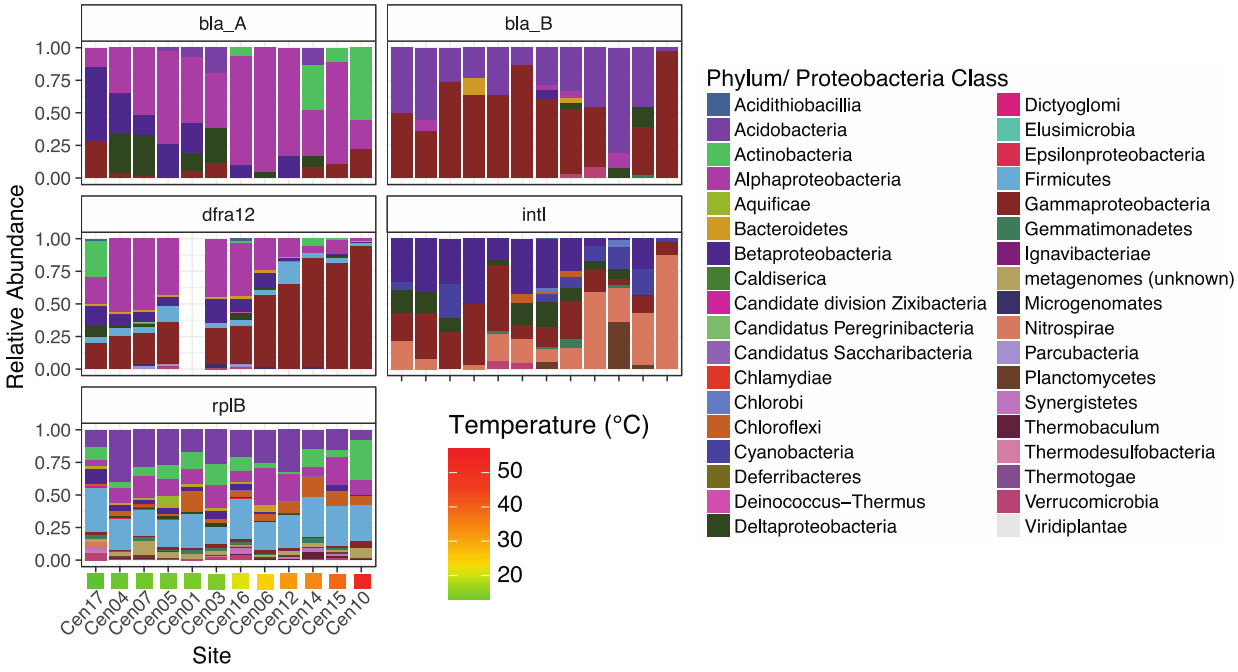

Supplementary Results

We recently reported changes in community structure in surface soils along the Centralia coal seam fire, and this conclusion was based on analysis of 16S rRNA gene amplicon data (Lee *et al.* 2017). In this work, we used *rplB* community structure to compare ARG profiles because both were determined by the same annotation and assembly methods from shotgun metagenomes. Thus, we first asked whether patterns observed using *rplB* sequences were similar to patterns we observed previously with 16S rRNA gene amplicons. Overall, patterns in community structure were consistent between these analyses (**Figure S2**). This was verified based on significant Mantel tests between *rplB* and 16S rRNA genes (Mantel's $r = 0.5877$, $p = 0.001$ on 999 permutations, at the OTU level. There was no relationship between spatial proximity of soils and *rplB* community structure (Mantel's $r = -0.14$, $p > 0.05$ on 999 permutations), confirming our previous report that community structure is not strongly driven by local dispersal. *rplB* evenness was negatively correlated with temperature ($\rho = -0.66$; $p < 0.05$), and *rplB* richness also trended negatively ($\rho = -0.55$; $p = 0.05$) (**Figure 2AC)**. Decreased alpha diversity with increased temperature was expected because of the complex and extreme fire stressor (e.g., exposure to high temperature and coal combustion pollutants, Janzen and Tobin-Janzen 2008), and, again, is in agreement with our previous study (Lee and Sorensen et al. 2017). The only obvious difference was that the *rplB* dataset had a greater abundance of Firmicutes than the 16S rRNA gene dataset, which may be due to differences in DNA extraction methods (Rubin *et al.* 2014) or marker gene target.

Figure S1. Sampling strategy along the Centralia temperature gradient. Twelve surface soils were collected along two fire fronts. Sampling sites are classified based on historical fire activity (Elick 2011) and observations of fire activity at the time of sampling: fire affected (red), recovered (yellow), and recovered (green, reference). Red bullseye indicates fire origin, and fire fronts one and two are indicated with arrows (F1 and F2, respectively).

Figure S2. Comparison of community structure assessed using two different methods. Community structure determined by *rplB* **(A)** is similar to previously described community structure determined by 16S rRNA gene sequencing reported in Lee and Sorensen et al. 2017**(B)**. Samples are classified by their fire history: fire affected (n = 6), recovered (n = 5), and reference (n = 1).

Figure S3. Pair-wise Spearman's correlations of normalized ARG abundances in Centralia. Spearman's rho is indicated in each cell and by color, where negative correlations are red and positive correlations are blue. False discovery rate adjusted significance is noted by asterisks.

Figure S4. Relationship between normalized abundance of ARGs and soil temperature. Point shape indicates soil fire classification. Coverage-adjusted abundance for each gene was normalized to total abundance of single copy gene *rplB*. Normalized abundance is plotted against soil temperature. Note the differences in y-axes. Shape indicates soil classification based on fire history.

Figure S5. Beta diversity of Centralia microbial communities with rplB and ARGs. Principal coordinate analysis (PCoA) based on weighted Bray-Curtis distances of community structure (**A**) and ARG structure (**B**). Colors represent soil temperature, and shape indicates soil classification based on fire history.